

Persistence exponents in a three-dimensional symmetric binary fluid mixture

V. M. Kendon,^{1,*} M. E. Cates,¹ and J.-C. Desplat²

¹*Department of Physics and Astronomy, JCMB King's Buildings, University of Edinburgh, Mayfield Road, Edinburgh EH9 3JZ, United Kingdom*

²*Edinburgh Parallel Computing Centre, JCMB King's Buildings, University of Edinburgh, Mayfield Road, Edinburgh EH9 3JZ, United Kingdom*

(Received 21 October 1999)

The persistence exponent, θ , is defined by $N_F \sim t^{-\theta}$, where t is the time since the start of the coarsening process and the “no-flip fraction,” N_F , is the number of points that have not seen a change of “color” since $t=0$. Here we investigate numerically the persistence exponent for a binary fluid system where the coarsening is dominated by hydrodynamic transport. We find that N_F follows a power law decay (as opposed to exponential) with the value of θ somewhat dependent on the domain growth rate ($L \sim t^\alpha$, where L is the average domain size), in the range $\theta = 1.23 \pm 0.1$ ($\alpha = 2/3$) to $\theta = 1.37 \pm 0.2$ ($\alpha = 1$). These α values correspond to the inertial and viscous hydrodynamic regimes, respectively.

PACS number(s): 82.20.Wt, 64.60.Ht, 64.75.+g

I. INTRODUCTION

Persistence exponents can be defined for systems where there is an order parameter whose time evolution can be followed at each point, \mathbf{x} , in the system. It is most easily understood for an order parameter, $\phi(\mathbf{x})$ that takes just two equilibrium values (spin up/down), but the concept is easily generalized (e.g., red/blue fluid for binary fluid mixtures). The density of points for which $\text{sgn}[\phi(\mathbf{x}) - \langle \phi \rangle]$ has not changed sign up to time t as the system coarsens, the “no-flip fraction,” N_F , will, for a conserved order parameter, or a quench to zero temperature, typically decay as a power law, $N_F \sim t^{-\theta}$, where θ is the persistence exponent.

Persistence exponents were first investigated by Bray, Derrida, and Godrèche [1,2], in the context of one-dimensional diffusive systems. For example, for the q -state Potts model in one dimension, Derrida *et al.* [2] found from simulations, and later proved analytically [3], that $\theta = 3/8$ for $q=2$, $\theta \approx 0.53$ for $q=3$, and $\theta \rightarrow 1$ as $q \rightarrow \infty$. It is also possible to define persistence exponents for systems with non-conserved order parameters at finite temperature by coarse graining [4].

As with most critical systems, analytical calculations are difficult; a few exact results exist [1,3]. Some mean field calculations have been done [5], however, mean field approximations also predict that θ is not independent of the other critical exponents. Mean field theory assumes that the order parameter dynamics is a Markov process, and Derrida *et al.* and Majumdar *et al.* [6,5] argue that, in general, this is not the case, and thus θ is, in fact, a new critical exponent independent of the four already known (two static exponents, the domain coarsening exponent, α , and the exponent for the critical slowing-down of the correlations as the critical point is reached from a mixed state [7]).

In this paper we present an investigation of the persistence behavior of our simulation of three-dimensional (3D)

spinodal decomposition in a binary fluid mixture, other results of which are reported elsewhere [8,9]. Brief details of the theoretical model and simulation method are given first, followed in Sec. III by a theoretical approach to persistence behavior in this system. In Sec. IV the numerical analysis is described, with the results for the flip rate given in Sec. V and estimates of the persistence exponent in Sec. VI. Finally, in Sec. VII, the results are summarized.

II. MODEL AND SIMULATION

A symmetric binary fluid mixture differs from a purely diffusive system, such as an alloy, in that the phase separation is assisted by hydrodynamics. There is an initial diffusive period during which an interlocking structure of single-fluid regions is formed, separated by sharp interfaces. The interfaces then take over as the driving force, displacing the fluid as they flatten and shrink, leading to a much more rapid domain growth rate of $L \sim t$ (in 3D) compared to diffusive growth of $L \sim t^{1/3}$, where L is the average domain size. This linear growth was first predicted by Siggia [10]. Furukawa [11] later predicted that as the inertial effects came into play, the growth rate would slow to $L \sim t^{2/3}$. These growth rates have been observed in simulation [8,12] and linear growth has been observed experimentally [13]. Recent suggestions that the growth rate may slow still further to $L \sim t^{1/2}$ (or slower) [14] are not supported by our simulation work [8] or theory [15], and will not concern us here.

For numerical work, we use the following model free energy:

$$F = \int d\mathbf{r} \left\{ -\frac{A}{2} \phi^2 + \frac{B}{4} \phi^4 + \tilde{\rho} \ln \tilde{\rho} + \frac{\kappa}{2} |\nabla \phi|^2 \right\}, \quad (1)$$

in which A , B , and κ are parameters that determine the interfacial width ($\xi = \sqrt{\kappa/2A}$), and interfacial tension [$\sigma = (8\kappa A^3/9B^2)^{1/2}$]. ϕ is the usual order parameter (the normalized difference in number density of the two fluid species); $\tilde{\rho}$ is the total fluid density, which remains (virtually) constant throughout [16,17]. We choose $A/B=1$ so $\phi =$

*Present address: Department of Physics and Applied Physics, University of Strathclyde, Glasgow G1 1XQ, United Kingdom.

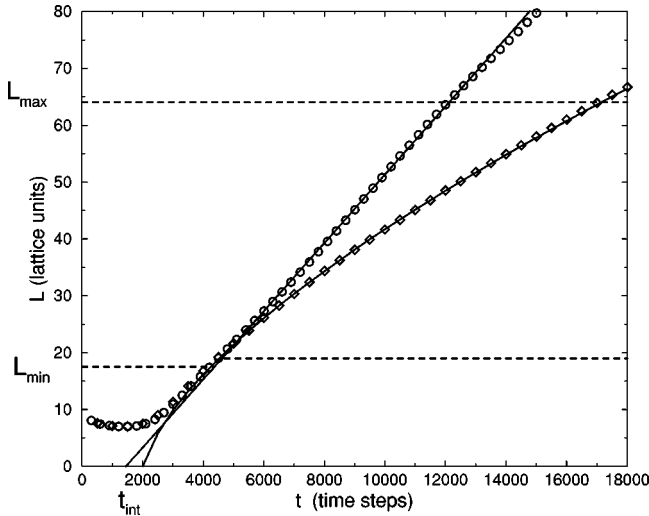


FIG. 1. L vs t for the runs with $L_0=5.9$ (circles) and 0.0003 (diamonds). The region used for fitting is delimited by $L_{\min} < L < L_{\max}=64$, and the fits (solid) (to $\alpha=1$ and $\alpha=2/3$, respectively) are projected back to show the intercepts, t_{int} .

± 1 in equilibrium. Our simulation [18] uses a lattice Boltzmann (LB) method [19,16] with a cubic lattice with nearest and next-nearest neighbor interactions (D3Q15). It was run on Cray T3D and Hitachi SR-2201 parallel machines with system sizes up to 256^3 .

The data used for the analysis of persistence behavior corresponds to that used in our earlier studies of the growth exponents [8]. Details of the simulation parameters for each run, and selection of usable data can also be found in Ref. [8]. The filters used to eliminate diffusive and finite size effects mean that the good data from any single 256^3 run lies within $20 \leq L \leq 64$ in units of the lattice spacing. The data was fitted to $L = b(t - t_{\text{int}})^\alpha$, where b is a prefactor determined by the physical parameters and t_{int} is a nonuniversal adjustment to the zero point on the time scale dependent on the initial diffusive period. Figure 1 shows two sample runs and the fitted curves. The values of α and t_{int} will be used in the subsequent analysis of the persistence behavior. By using characteristic length [$L_0 = \eta^2 / (\rho\sigma)$] and time [$t_0 = \eta^3 / (\rho\sigma^2)$] scales uniquely defined by the physical parameters, the data from all the runs was combined into a single L, t plot covering a linear region, through a broad crossover, to $t^{2/3}$ [8]. The value of the growth exponent, α , where the domain size, $L \sim t^\alpha$, was found to range from 1.0 to 0.67, thus the data spans the full range from viscous to inertial hydrodynamic growth. The breadth of the crossover region justifies the use of a single effective exponent, α , to fit any single run. It is convenient to use the value of L_0 (in simu-

lation units) to distinguish the different simulation runs. The viscous regime corresponds to $L_0 > 1$, the inertial regime to $L_0 < 0.001$, with intermediate values corresponding to the crossover region.

III. FLIP-RATE MODEL

For the 3D binary fluid system it is unrealistic to expect to derive anything but the simplest approximate results using a theoretical approach. However, this will serve to illuminate the persistence-related quantities under discussion. The simple results to be derived in this section will then be of assistance in the numerical analysis that follows.

Consider the step by step ($\Delta t = 1$ in simulation units) time evolution of the value of the order parameter at a single point as the system phase separates and coarsens from the initially completely mixed state. A typical example is represented schematically in Fig. 2. In order to focus on the behavior in the hydrodynamic regime, an initial state is chosen at a reference point, t_{start} , a time corresponding to when domains have coarsened to a size $L \sim L_{\min}$ that marks the onset of purely hydrodynamic behavior (determined by the point at which diffusive growth has fallen below 2% [8]). The ‘‘no-flip fraction,’’ $N_F(t/t_{\text{start}})$ is then defined as the fraction of sites that have not changed color since t_{start} . Scaling by t_{start} is equivalent to choosing units such that $t_{\text{start}} = 1$, which is in any case the value of the initial reference time used in other studies.

In order to derive an approximate functional form for $N_F(t/t_{\text{start}})$, it is useful to define two further quantities, (i) the flip rate, $P_F(t)$ is simply the proportion of sites that changed color between time step $t-1$ and t , and, (ii) the flip probability, $P(t, t_1)$, is the probability that a site changes color at time t , given that it last changed color at time t_1 .

These two quantities are related as follows:

$$P_F(t) = \int_{t_{\text{int}}}^t dt_1 P_F(t_1) P(t, t_1), \quad (2)$$

where the sum over discrete time in our simulations has been approximated by an integral. Equation (2) says that the flip rate at time t is given by all the points that last flipped at time t_1 and are due to flip again at time t , i.e., $P(t, t_1)$, integrated over all possible prior flip times, $t_{\text{int}} < t_1 < t$, and weighted by the number of sites with prior flip time t_1 , i.e., $P_F(t_1)$. The lower limit of the integral is set to t_{int} because, as can be seen from Fig. 1, t_{int} corresponds to the natural zero point on the time scale, the time at which (ignoring diffusion and the finite width of the interfaces), the domain size would be zero

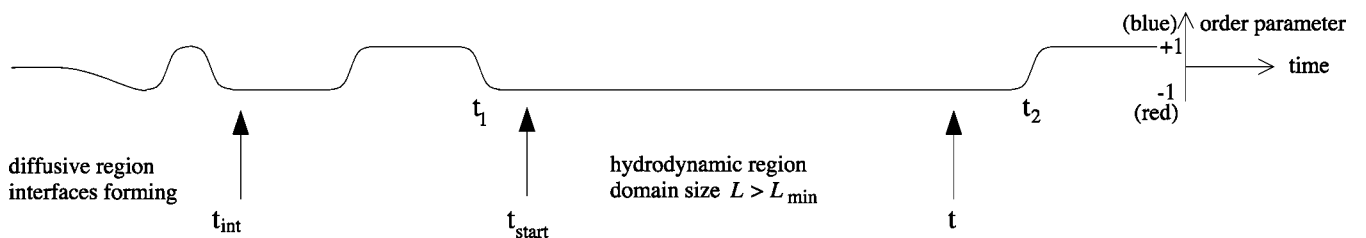


FIG. 2. Persistence timeline.

so that, in effect, every site flipped at $t=t_{\text{int}}$. Henceforth t_{int} will be usually be set to zero, to simplify the algebra.

Equation (2) is an integral equation in two unknown functions, $P(t, t_1)$ and $P_F(t)$. A solution for $P(t, t_1)$ can be obtained by making some assumptions about the asymptotic form of the simpler quantity, $P_F(t)$, for the 3D hydrodynamic system. The dynamics are determined by the basic scaling growth law, $L=b(t-t_{\text{int}})^\alpha$, where the prefactor b depends on the system parameters (density, viscosity, interfacial tension). Once the initial diffusive period is over, and the domains of red and blue fluid are separated by well-formed interfaces, lattice sites change color from red to blue when an interface moves across them as the domains grow in size. The flip rate, $P_F(t)$, is thus given by the rate at which the interface moves through the system sweeping out a volume of points that change color. So, an estimate of the area of the interface, and its average speed, will yield an estimate for $P_F(t)$. This is the ‘‘flip-rate model.’’

The area of the interface is given approximately by $A(t) = c_L V/L$, where V is the system volume and c_L is a prefactor of order unity. As the system coarsens, the interfaces must move to accommodate the enlargement of the domains. So long as there is only one length scale in the domain structure, the speed at which the interface moves will be of order dL/dt . Also, it has been shown [9] that the average fluid velocity is comparable in magnitude with dL/dt , so the speed of the interface can be estimated by $c_v dL/dt$, where c_v is another prefactor of order unity. The volume swept out per unit time will be $A(t) c_v dL/dt$. Combining both c_L and c_v into a single prefactor, c , the flip rate per unit volume will be approximately,

$$P_F(t) = c \frac{1}{L} \frac{dL}{dt} = \frac{c\alpha}{t}. \quad (3)$$

This approximation for $P_F(t)$ diverges at $t=0$. In the discrete time of our simulations, we start with time step $t=1$ so no divergences arise; in the continuum approximations it is appropriate to start at time $t=0$, thus we will need to take care that no integrals diverge at their lower limits.

Substituting $P_F(t) = c\alpha/t$ into Eq. (2) gives

$$\int_0^t dt_1 \frac{t}{t_1} P(t, t_1) = 1, \quad (4)$$

where we have set $t_{\text{int}}=0$. Equation (4) has solutions for $P(t, t_1)$ of the form

$$P(t, t_1) = (\beta-1)t_1^{\beta-1}t^{-\beta}, \quad \beta > 1, \quad (5)$$

where β is an arbitrary exponent, as can readily be verified by substitution. We have $P(t, t_1) \rightarrow 0$ for $t_1 \rightarrow 0$ so the integral is well behaved at $t_1=0$. The condition,

$$\int_{t_1}^{\infty} dt P(t, t_1) = 1, \quad (6)$$

(i.e., all sites do, eventually, flip) is also satisfied, so $P(t, t_1)$ is a properly normalized probability.

An expression can now be written down for the ‘‘no flip fraction,’’ $N_F(t/t_{\text{start}})$, which is the fraction of sites that have not changed color since t_{start} ,

$$N_F = \int_0^{t_{\text{start}}} dt_1 \int_t^{\infty} dt_2 P(t_2, t_1) P_F(t_1), \quad (7)$$

i.e., we count every point whose last flip was before t_{start} and whose next flip is after time t . Substituting for P_F and $P(t_2, t_1)$ gives,

$$\begin{aligned} N_F &= c\alpha \int_0^{t_{\text{start}}} dt_1 (\beta-1)t_1^{\beta-2} \int_t^{\infty} dt_2 t_2^{-\beta}, \\ &= \frac{c\alpha}{\theta} \left(\frac{t_{\text{start}}}{t} \right)^\theta, \quad \theta > 0, \end{aligned} \quad (8)$$

setting $\theta = (\beta-1)$ as the persistence exponent. The flip-rate model has thus provided an expression for N_F that has the exponent, θ , in the prefactor as well as being the asymptotic power of the decay. This puts helpful constraints on the data analysis, although for it to be really useful, the prefactor, c , in Eq. (3) has to be pinned down as precisely as possible. In a log-log plot,

$$\log N_F = \log(c\alpha/\theta) - \theta \log(t/t_{\text{start}}), \quad (9)$$

so plotting N_F against t/t_{start} should give a straight line when viewed log-log, with slope $-\theta$, for $t \gg t_{\text{start}}$. The initial data near $t \approx t_{\text{start}}$ will depart from this asymptotic behavior and tend to $N_F=1$ because by definition nothing flipped yet for $t=t_{\text{start}}$. The fit to the asymptotic slope should, however, have an intercept at $c\alpha/\theta$ for $t=t_{\text{start}}$.

It is possible to go on to define a hierarchy of persistence quantities, of which N_F is the first [2]. The ‘‘one flip fraction,’’ O_F is the density of points that have changed color exactly once since time t_{start} . Within the flip-rate model, an expression for O_F for this system can be derived in the same way as for N_F ;

$$\begin{aligned} O_F(t/t_{\text{start}}) &= \int_t^{\infty} dt_2 \int_{t_{\text{start}}}^{t_2} dt_f \int_0^{t_{\text{start}}} dt_1 P(t_2, t_f) \\ &\quad \times P(t_f, t_1) P_F(t_1). \end{aligned} \quad (10)$$

The ‘‘one flip’’ occurs at time t_f with $t_{\text{start}} < t_f < t_2$. The probability of an initial flip at t_1 with $0 < t_1 < t_{\text{start}}$, then flipping at time t_f is $P(t_f, t_1)$. The probability of flipping again at time t_2 is then $P(t_2, t_f)P(t_f, t_1)$, provided the two flip events are independent of each other (so the probabilities can be multiplied). In other words, this model assumes that the flip probability $P(t_2, t_f)$ is only dependent on the last time the site flipped, so it has no memory of earlier flips. This requires a Markov process for the coarsening dynamics, which Derrida *et al.* and Majumdar *et al.* [6,5] claim is not generally the case for the nonhydrodynamic systems they have considered. This therefore constitutes another untested assumption in the flip-rate model described here. Substituting for P_F and $P(t_2, t_1)$ as before gives

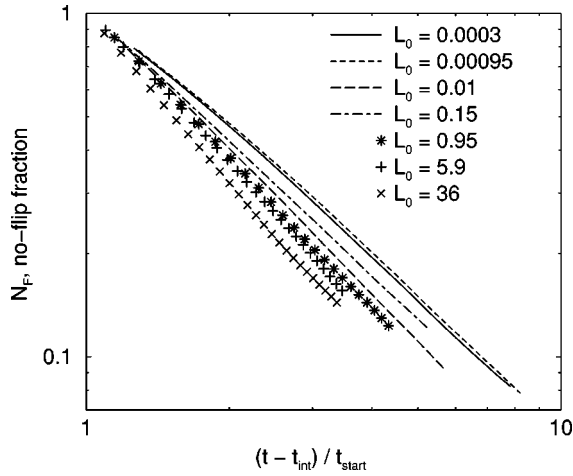


FIG. 3. No-flip fraction, N_F , for all runs.

$$O_F = \int_t^\infty dt_2 \int_{t_{\text{start}}}^{t_2} dt_f \int_0^{t_{\text{start}}} dt_1 \frac{c\alpha}{t_1} \theta \frac{t_f^\theta}{t_2^{\theta+1}} \theta \frac{t_1^\theta}{t_f^{\theta+1}} \quad (11)$$

$$= \frac{c\alpha}{\theta} \left(\frac{t_{\text{start}}}{t} \right)^\theta \left[1 - \ln \left(\frac{t_{\text{start}}}{t} \right) \right],$$

after integrating by parts. This has a dominant logarithmic term so it does not have an asymptotic power law decay. (In contrast, in the 1D Ising model, O_F appears to have the same asymptotic behavior as N_F , see Refs. [2,3].) This could, of course, be a result of the limitations of the flip-rate model, however, the simulation results suggest that the asymptotic behavior of O_F is different from that of N_F (see Figs. 3 and 4). Again, this expression is only valid for $t \gg t_{\text{start}}$ since $O_F \rightarrow 0$ for $t \rightarrow t_{\text{start}}$. As with N_F , the (same) critical exponent θ appears both as an exponent and as a prefactor, thus providing an extra constraint on any fits to simulation data.

Nothing in the theory so far is specific to three space dimensions. However, in two-dimensional binary fluid systems, the interface does not completely interconnect [20], so the approximation $P_F = c\alpha/t$ is unlikely to work without modification. Furthermore, 2D hydrodynamic coarsening shows nonscaling features [20] which make the analysis

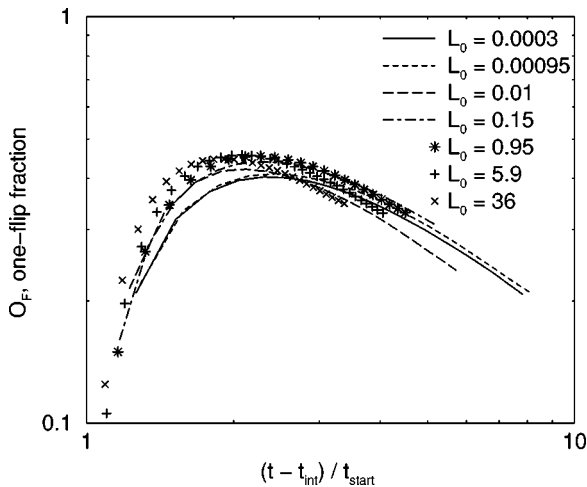


FIG. 4. No-flip fraction, O_F , for all runs.

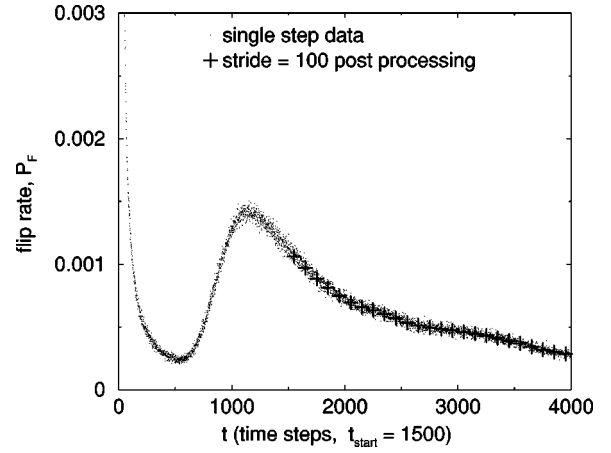


FIG. 5. Flip rate, P_F , for a 96^3 system, single step (dots) and $\Delta t_{\text{stride}} = 100$ steps (crosses).

more complicated and difficult to interpret both theoretically and numerically. Therefore, since our main work is with the three-dimensional system, the two-dimensional form of the theory will not be pursued further here.

IV. NUMERICAL ANALYSIS

The flip-rate model just described will now be used to guide the analysis of the data from our spinodal decomposition simulations. The data from the largest (256^3) runs is typically saved every 200 to 500 time steps, Δt_{stride} . It is also coarse grained from a 256^3 lattice down to 128^3 by averaging over groups of eight neighboring lattice points. This data can be used to calculate the four key quantities discussed in the previous section, P_F , $P(t_1, t_2)$, N_F , and O_F , provided the spatial and temporal coarse graining makes no significant difference to the results.

To investigate temporal coarse graining, a special run on a 96^3 grid was done with the key quantities calculated every time step. This extra computation significantly slows down the computer run time so it is not practical to perform larger simulations with single-step calculations. The results from a single-step calculation were then compared with the same run analyzed over a stride of 100 time steps, see Fig. 5. The result of this comparison showed excellent agreement between the single-step and strided estimates of $P_F(t)$. In fact, the errors introduced by analyzing only every Δt_{stride} steps rather than every single step arise from miscounting sites that flip more than once in that period. If the flip rate, $P_F(t)$, is small then the number of multiple flips will be much smaller still, so the errors will be negligible. In all runs analyzed, P_F was found to be small even over the largest Δt_{stride} used, i.e., $P_F \Delta t_{\text{stride}} \ll 1$ (a value of 1 would mean every site flipped).

The shape of $P_F(t)$ in Fig. 5 for times $t < t_{\text{start}}$ clearly shows a transition from diffusive to hydrodynamic behavior in the initial fall (diffusion), rise (interfaces start to move), and fall again (hydrodynamic). Thus $P_F(t)$ is a sensitive indicator of the system dynamics, and the choice of $t_{\text{start}} = 1500$ in this 96^3 system is confirmed to be located, as desired, near the beginning of the hydrodynamic regime but

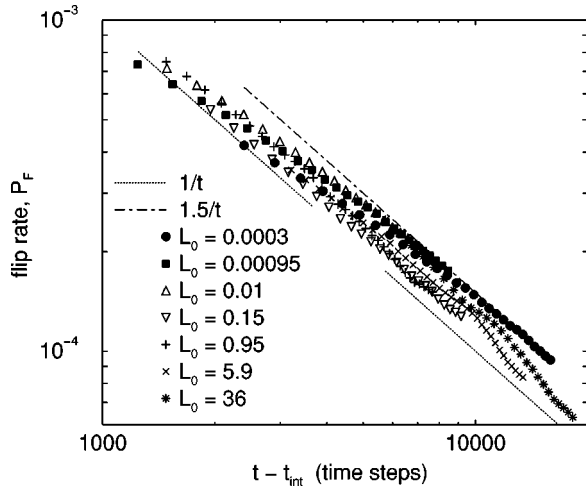


FIG. 6. Flip rate, P_F , for simulation runs as identified by L_0 values in key, log-log plot. Also shown for comparison, $1/t$ and $1.5/t$.

not too close to the transition from diffusive behavior. The effect of spatial coarse graining was checked by comparing the results of analyzing strided data from 128^3 and 256^3 runs with identical parameters apart from system size. Excellent agreement was found everywhere except in the tail of $P(t, t_{\text{start}})$, which can be explained by poor statistics in this region. The conclusion, therefore, is that spatial and temporal coarse graining on the scale used in this analysis does not introduce significant errors into the results.

From the main simulation data, good statistics for P_F , N_F , and O_F can be obtained, as every lattice point can be assessed according to if/when it next flips after t_{start} . The statistics are not so good for estimating $P(t, t_{\text{start}})$, because the reference base is reduced to only those sites that flip between t_{start} and Δt_{stride} rather than the whole system; recall that $P(t, t_{\text{start}})$ refers to the first flip happening exactly at t_{start} .

V. FLIP RATE

In order to make full use of the model presented in Sec. III, it is necessary to investigate whether the flip rate really follows the approximate theoretical expression, $P_F = c\alpha/t$, Eq. (4), and whether the prefactor, c , can be evaluated sufficiently accurately from the simulation data to allow a strongly constrained fit to be done for θ in the analysis of N_F and O_F . Figure 6 shows P_F for each simulation run in a log-log plot, with $1/t$ and $1.5/t$ also shown for comparison. The prefactor, c , clearly varies somewhat over time, and with α , although the variation with time can partly be explained since early times, $t \sim t_{\text{start}}$, are expected to differ from asymptotic behavior.

To determine the values and variation in c more accurately, a linear plot of the flip rate, P_F , scaled by $(t - t_{\text{int}})/\alpha$ is shown in Fig. 7. It can be seen that the results roughly split into two groups corresponding to the runs found to be in the viscous and lower crossover regions ($L_0 \geq 0.1$), with prefactors around $c \approx 1.25$, and runs in the inertial regime ($L_0 \leq 0.01$), with $c \approx 2.2$.

TABLE I. Summary of results for c and θ .

L_0	α	c	θ
0.0003	0.67	1.5 – 1.9	1.20 – 1.23
0.00095	0.67	1.5 – 2.2	1.20 – 1.32
0.01	0.75	1.3 – 1.9	1.25 – 1.40
0.15	0.80	1.0 – 1.5	1.15 – 1.24
0.95	0.95	0.85 – 1.4	1.20 – 1.40
5.9	1.0	0.85 – 1.4	1.25 – 1.50
36	1.0	0.85 – 1.3	1.30 – 1.55

If this difference in the value of c is real, it implies that the geometry of the separating domains is different between the viscous and inertial regimes. Any such difference is not apparent to the eye in visualizations of the interface [21]. There is some evidence from analysis of the structure factor [9] that there is a structural difference in the domain structure, but it is unclear whether this is enough to account for the observed difference in the value of c . However, there is another possible interpretation of the data, which is that the flip rate actually exceeds $c\alpha/t$ for the inertial regime runs. For once the viscosity is low enough for inertial effects to become significant, the interface may exhibit capillary excitations. This oscillation of the interface could increase the measured flip rate as sites near the interface repeatedly flip back and forth, but without contributing to the sweeping that removes sites from the “no flip” category. If capillary excitations have a significant effect on the flip rate, this part of the flip rate needs to be discounted in the subsequent fitting to determine the persistence exponent. Since the extent of any excess flip rate cannot be determined at this stage, a variable prefactor, c , has therefore been carried through the fitting process for θ .

VI. PERSISTENCE EXPONENT

The “no flip fraction,” N_F , is the primary quantity of interest in this work, being the quantity from which the persistence exponent θ , is defined, $N_F \sim t^{-\theta}$. The simulation results for N_F , with the time scaled as $(t - t_{\text{int}})/t_{\text{start}}$ and points

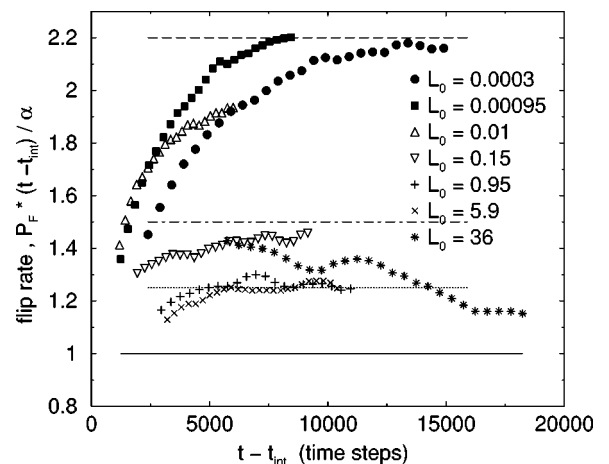


FIG. 7. Flip rate, P_F , rescaled by $(t - t_{\text{int}})/\alpha$ on a linear plot so values of the prefactor, c , can be read off the ordinate axis.

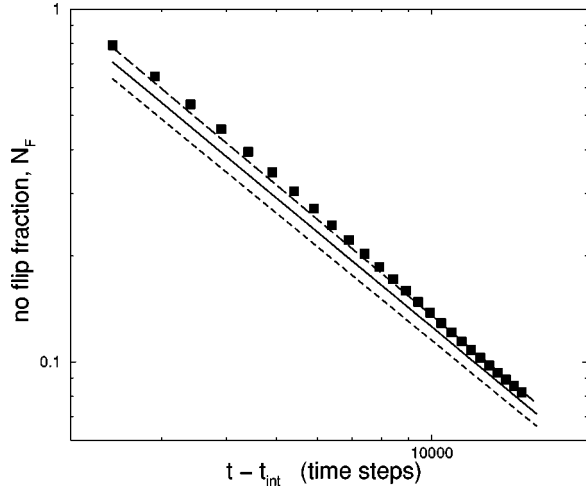


FIG. 8. Fitted curves for N_F for the run with $L_0=0.0003$. The no flip fraction N_F (squares) calculated from the numerical data is shown with the upper, median, and lower fits to Eq. (8) using, respectively, $c=1.9$, $\theta=1.23$ (dashed line); $c=1.7$, $\theta=1.215$ (solid line); and $c=1.5$, $\theta=1.21$ (dotted line); from Table I.

for times at which $L < L_{\min}$ or $L > 64$ removed, are plotted in Fig. 3. The runs in the inertial regime have tails that fall to around $N_F=0.08$, while the viscous runs stop (reach domain size $L=64$) at around $N_F=0.15$. There is thus barely one decade within which to estimate the slope of the tail. Although a simple linear fit cannot produce a very accurate result, superficial inspection suggests that θ is slightly greater than unity, and fairly reproducible.

If we could use a fixed value of the prefactor, c , with confidence, the fit could be constrained to intercept at $c\alpha/\theta$, Eq. (9). Instead, a family of fits was done [21], covering a range of values of the prefactor, c , and these were compared with a similar family of fits for the one flip fraction, O_F . As can be seen in Fig. 4, O_F at best falls to only 0.2 by the end of the simulation data, so it cannot be regarded as having reached asymptotic behavior yet. The O_F data was therefore used only to confirm the direction in which N_F is tending towards its asymptote. From this fitting procedure, a range of consistent values of both c and θ were obtained, and these are summarized in Table I.

A sample plot for the run with $L_0=0.0003$ with N_F and the fitted expression in Eq. (8), with high, median, and low values of c and θ , is shown in Fig. 8. Fits to $P(t, t_{\text{start}}) = \theta/t(t_{\text{start}}/t)^\theta$ were also done, producing values of θ consistent with those determined from N_F and O_F . Since $P(t, t_{\text{start}})$ does not depend on c or α , this is a useful check for consistency, but because of the poorer statistics for $P(t, t_{\text{start}})$, no improvement in the range of values for θ was obtained by this extra step.

The complete set of estimates for θ from Table I is shown against the growth exponent α in Fig. 9, with error bars indicating the range of values obtained. The results are consistent with the persistence exponent, θ , lying somewhere around 1.37 for the viscous regime and 1.23 for the inertial regime. A single value of $\theta=1.333$ is also just about consistent with the data, although some variation with α seems more likely.

The prefactor, c , could be as low as 1.0 for viscous runs

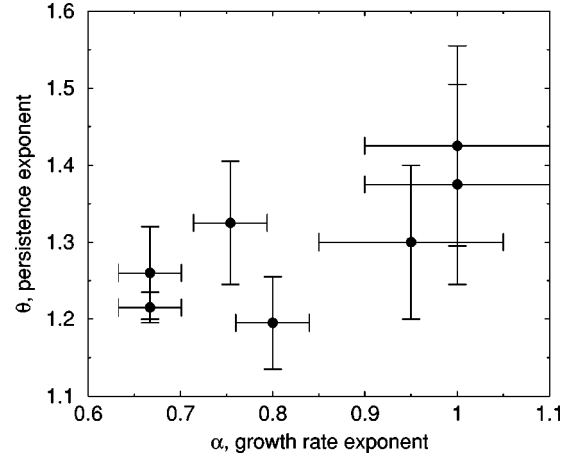


FIG. 9. Persistence exponent, θ , against spinodal growth rate exponent, α , from simulation runs. The error bars are the range of θ from Table I, and the error estimates for α of 10% (viscous regime) and 5% (crossover and inertial regime) [9].

and rises nearer to 2.0 for the inertial regime. However, a value of $c=2.2$ as implied by the measured flip rate for the inertial regime appears to be inconsistent with the persistence data for N_F , O_F , and $P(t, t_{\text{start}})$. The flip rate is thus sufficiently sensitive to distinguish between viscous and inertial regime dynamics, and suggests the presence of some mechanism such as capillary waves in the inertial regime that raises the measured flip rate above that predicted by the growth of the domains.

VII. CONCLUSIONS

In this investigation of the persistence exponents for a 3D hydrodynamic spinodal system, it has been observed that the decay of the ‘‘no-flip fraction,’’ N_F , is a power law (as opposed to exponential). It has not been possible to produce a very accurate determination of the persistence exponent, θ , but limits have been placed on the likely value, and it has been shown that some variation with the effective growth exponent, α , as one crosses slowly from viscous ($\alpha=1$) to inertial ($\alpha=2/3$) coarsening, should be allowed for in any future studies. The best estimate of θ for the viscous regime ($\alpha=1$), is $\theta=1.37\pm 0.2$. From the point of view of fundamental critical exponents, the value of θ in the inertial regime is perhaps more significant, since this is (at least on current evidence) the asymptotic behavior for spinodal decomposition, and here the best estimate is $\theta=1.23\pm 0.1$. These represent the first estimates of θ in a system dominated by hydrodynamics rather than diffusion. However, the error limits quoted here do not allow for systematic errors arising from the use of the flip-rate model itself. More accurate determination from simulations would likely require significantly larger system sizes, which is difficult to envisage at present computing power.

ACKNOWLEDGMENTS

We thank Alan Bray for drawing our attention to this problem, and Martin Evans for valuable discussions. This work was funded in part by EPSRC GR/M56234.

- [1] A. J. Bray, B. Derrida, and C. Godrèche, *Europhys. Lett.* **27**, 175 (1994).
- [2] B. Derrida, A. J. Bray, and C. Godrèche, *J. Phys. A* **27**, L357 (1994).
- [3] B. Derrida, V. Hakim, and V. Pasquier, *Phys. Rev. Lett.* **75**, 751 (1995).
- [4] S. Cueille and C. Sire, *Eur. Phys. J. B* **7**, 111 (1999) (in general, N_F defined for a single site in a system with nonconserved order parameter will decay exponentially at finite temperature due to thermal noise).
- [5] S. N. Majumdar, A. J. Bray, S. J. Cornell, and C. Sire, *Phys. Rev. Lett.* **77**, 3704 (1996).
- [6] B. Derrida, V. Hakim, and R. Zeitak, *Phys. Rev. Lett.* **77**, 2871 (1996).
- [7] H. K. Janssen, B. Schaub, and B. Schmittman, *Z. Phys. B* **73**, 539 (1989); D. A. Huse, *Phys. Rev. B* **40**, 304 (1989).
- [8] V. M. Kendon, J.-C. Desplat, P. Bladon, and M. E. Cates, *Phys. Rev. Lett.* **83**, 576 (1999).
- [9] V. M. Kendon, M. E. Cates, J.-C. Desplat, I. Pagonabarraga, and P. Bladon (unpublished).
- [10] E. D. Siggia, *Phys. Rev. A* **20**, 595 (1979).
- [11] H. Furukawa, *Phys. Rev. A* **31**, 1103 (1985).
- [12] See, e.g., M. Laradji, S. Toxvaerd, and O. G. Mouritsen, *Phys. Rev. Lett.* **77**, 2253 (1996); C. Appert, J. F. Olson, D. H. Rothman, and S. Zaleski, *J. Stat. Phys.* **81**, 181 (1995); T. Lookman, Y. Wu, F. J. Alexander, and S. Chen, *Phys. Rev. E* **53**, 5513 (1996); S. Bastea and J. L. Lebowitz, *Phys. Rev. Lett.* **78**, 3499 (1997); S. I. Jury, P. Bladon, S. Krishna, and M. E. Cates, *Phys. Rev. E* **59**, R2535 (1999).
- [13] See, e.g., K. Kubota, N. Kuwahara, H. Eda, and M. Sakazume, *Phys. Rev. A* **45**, R3377 (1992); S. H. Chen, D. Lombardo, F. Mallamace, N. Micali, S. Trusso, and C. Vasi, *Prog. Colloid Polym. Sci.* **93**, 331 (1993); T. Hashimoto, H. Jinnai, H. Hasegawa, and C. C. Han, *Physica A* **204**, 261 (1994).
- [14] M. Grant and K. R. Elder, *Phys. Rev. Lett.* **81**, 14 (1999).
- [15] V. M. Kendon (unpublished).
- [16] M. R. Swift, E. Orlandini, W. R. Osborn, and J. Yeomans, *Phys. Rev. E* **54**, 5041 (1996).
- [17] A. J. Ladd, *J. Fluid Mech.* **271**, 285 (1994).
- [18] J.-C. Desplat, I. Pagonabarraga, and P. Bladon (unpublished).
- [19] F. J. Higuera, S. Succi, and R. Benzi, *Europhys. Lett.* **9**, 345 (1989).
- [20] A. J. Wagner and J. M. Yeomans, *Phys. Rev. Lett.* **80**, 1429 (1998).
- [21] V. M. Kendon, Ph.D. thesis, Edinburgh University, 1999.